Potassium titanate nanowires: Structure, growth, and optical properties

G. H. Du,[1] Q. Chen,[2] P. D. Han,[1,3] Y. Yu,[1,3] and L. -M. Peng[1,2,*]
[1]*Beijing Laboratory of Electron Microscopy, Chinese Academy of Sciences, P.O. Box 2724, Beijing 100080, China*
[2]*Department of Electronics, Peking University, Beijing 100871, China*
[3]*College of Material Science and Technology, Taiyuan University of Technology, Taiyuan 030024, China*
(Received 6 June 2002; published 30 January 2003)

A simple one step hydrothermal reaction among TiO_2 nanoparticles and KOH solution was found to result in potassium titanate nanowires. The diameters of these nanowires are about 10 nm and the lengths range from 500 nm to 2 μm. The nanowires were analyzed by a range of methods including powder x-ray diffraction (XRD), high resolution electron microscopy (HREM), selected area electron diffraction, electron energy loss spectroscopy, XRD and HREM image simulations. The structure of the nanowires is determined to be of the type of $K_2Ti_6O_{13}$. Based on HREM observations of the growth process of the nanowires, we propose that the growth of the namowire was initiated by the formation of the $K_2Ti_6O_{13}$ nuclei inside the anatase matrix following the crystallographic relation $(200)_{\text{nanowire}}//(101)_{\text{anatase}}$. These nuclei subsequently grew to form one-dimensional nanowires via preferential growth along the [010] direction. Absorption experiments show that the potassium titanate nanowires are wide-band semiconductors with a band width $E_g \sim 3.45$ eV.

DOI: 10.1103/PhysRevB.67.035323 PACS number(s): 81.07.De, 81.07.Vb, 81.07.Bc

I. INTRODUCTION

One-dimensional semiconducting nanostructures, such as nanotubes and nanowires, have attracted a wide rang of interest because of their remarkable electronic, magnetic, optical, catalytic, and mechanical properties which are different from that of the bulk materials, and these nanostructures may eventually leads to applications in nanodevices.[1–3] Among these semiconducting nanomaterials, titanate is a wide band semiconductor having many important applications in areas such as photocatalysts, gas sensors, and high effect solar cells[4] Titanate nanotubes and nanowires are particularly interesting partly because they have large specific surface and may enhance the photocatalytic activity, leading to a higher potential of applications in environmental purification, decomposition of carbonic acid gas and generation of hydrogen gas.[5,6] In other fields titanate whiskers have been shown to have high chemical and thermal stability and potential applications in whisker-reinforced plastics and metals.[7,8] Many methods have been developed to synthesize titanate whiskers, including calcination, flux growth, and melting reaction,[9] but typically the diameters of the obtained products were in micrometer scale. In an earlier paper we described a simple hydrothermal method for preparing titanate nanotube by reacting TiO_2 with NaOH solution.[10] More recent studies show that nanowire products with narrow diameter distribution around 10 nm and lengths ranging from 500 nm up to 2 μm can be obtained if NaOH is replaced by KOH. In this paper we report an investigation on the structure, growth mechanism, and optical property of the nanowires. We will show that these nanowires have the same structure as the potassium hexatitanate ($K_2Ti_6O_{13}$) (which belongs to the family of $K_2Ti_nO_{2n+1}$, with $3 \leqslant n \leqslant 6$), and have a wide band gap of about 3.45 eV.

II. EXPERIMENTAL

Our nanowire samples were prepared by hydrothermal method. Commercially bought TiO_2 ($>99\%$ pure anatase phase) was used as the raw material. About 0.3 g raw powder material was added to 35 ml KOH (10M) aqueous solution and the mixture was then heated at 130 °C in Teflon-lined stainless steel autoclaves for 3 days. The nanowire products were obtained by filtering and washing the products with deionized water.

Powder x-ray diffraction (XRD) were performed with a Rigaku D/max 2400 diffractometer using monochromatic CuK_{α_1} radiation ($\lambda = 1.54$ Å) and scanning between 5° and 70° (2θ). Transmission electron microscopy (TEM) studies were performed using a high-resolution transmission electron microscope JEOL 2010 and a field-emission gun (FEG) transmission electron microscope Philips CM200/FEG, both operated at 200 kV. Electron energy loss spectroscopy (EELS) experiments were performed using the Gatan image filtering (GIF) system attached to the Philips CM200FEG. TEM specimens were prepared by dispersing the nanowire sample in alcohol followed by ultrasonic treatment. The sample was then dropped onto a holey carbon film supported on a copper grid and dried in air. XRD and high-resolution electron microscopy (HREM) simulations were carried out using the CERIUS2 software and a SGI 2100 computer workstation.

III. RESULTS

A. Structure

1. TEM and EELS

Figure 1(a) is a low magnification TEM image showing that the product contains a large quantity of nanowires with narrow size distribution. The diameters of the nanowires are uniform and around 10 nm and the lengths range from 500 nm up to 2 μm. To investigate the shape of the product, a single nanowire is selected and tilted along its axis. It is observed that the nanowire does not have a perfect circular cross section perpendicular to its axis. Instead it is better to describe the cross-section as a rectangle having rounded cor-

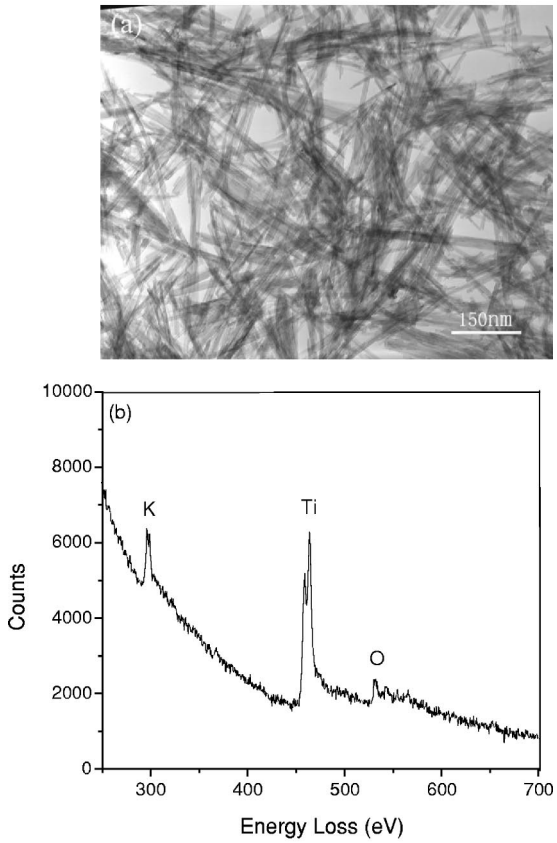

FIG. 1. (a) Low magnification TEM image showing nanowires with narrow diameter distribution and (b) electron energy loss spectroscopy spectrum recorded from a single free-standing nanowire.

ners. The length ratio between the long edge and the shorter edge is about 1.5 which will become clearer in our following discussions that the shorter edge is along the *c* axis of a layered structure. The composition of a single nanowire is analyzed using the technique of electron energy loss spectroscopy (EELS). Shown in Fig. 1(b) is a typical EELS spectrum obtained from a single free-standing nanowire. This EELS spectrum shows clearly the O *K* edge at 532 eV, the L_2 and L_3 edges of K at 297 and 294 eV, and that of Ti at 461 and 455 eV, respectively, suggesting that the nanowire is composed of mainly K, Ti, and O.

2. XRD and simulations

XRD experiments were performed and simulations were carried out in order to determine the structure of the nanowires. Figure 2(a) is a XRD profile taken from the raw TiO_2 sample showing that the raw sample is composed of almost pure anatase phase TiO_2. The XRD profile taken from the nanowire sample is shown in Fig. 2(b). The XRD profile taken from the nanowire sample is seen to be very different from that shown in Fig. 2(a), but a thorough search of structural datebases reveals that this profile may be indexed based on the structure of $K_2Ti_6O_{13}$ (monoclinic structure with $a=15.593$ Å, $b=3.796$ Å, $c=9.108$ Å, and $\beta=99.78°$).[11] For comparison XRD profiles from bulk and nanoscale $K_2Ti_6O_{13}$ crystals are calculated using CERIUS2 software and

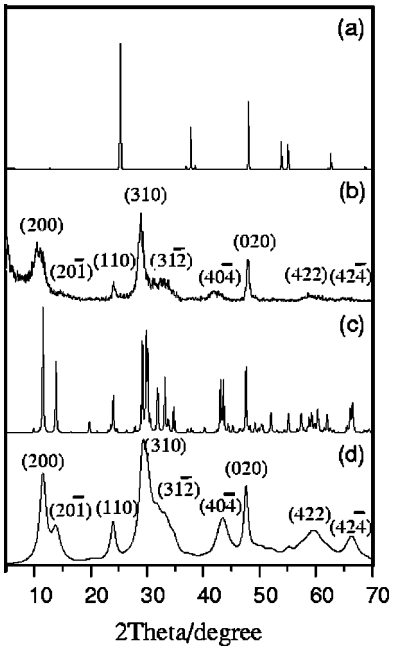

FIG. 2. Experimental XRD profiles recorded from (a) raw TiO_2 sample and (b) nanowires sample, and calculated XRD for (c) a perfect crystalline $K_2Ti_6O_{13}$ and (d) a $K_2Ti_6O_{13}$ nanawire.

the results are shown in Figs. 2(c) and 2(d). The peak positions of Figs. 2(b) and 2(c) are basically the same, but the peaks resulting from nanowires are broader and some peaks are overlapping with each other due to the nanometer size of the nanowires. Reasonable agreement between the experimental and simulated XRD profiles have been achieved. The residual discrepancy between these profiles might result from the presence of possible impurities in the sample, finite strain stored in the nanowire and possible lattice relaxation toward the surface of the nanowire where a high density of dangling bonds are expected.

3. Selected area electron diffraction

Using a selected area electron diffraction (SAED) aperture, an area ($\sim$200 nm in diameter) containing only nanowires can be selected and other effects due to impurity and/or multiphase may be avoided. Figure 3 shows a SAED pattern taken from an area containing many nanowires. This SAED pattern is basically a ring pattern, and like XRD profile this ring pattern can be indexed using $K_2Ti_6O_{13}$ crystal structure. Using SAED patterns taken from a single nanowire, we found that the growth direction of the $K_2Ti_6O_{13}$ nanowire is along [010], and this agrees with the growth of hexatitanate whiskers prepared by calcination.[12]

4. HREM and simulations

The atomic structure of the nanowires is further investigated using HREM. Figure 4 is a HREM image of the nanowire sample showing that the nanowires are basically layer-structured with a layer spacing of 7.7 Å. This distance corresponds to the (200) plane spacing of $K_2Ti_6O_{13}$.

To verify the structure of the nanowires, HREM image simulations were carried out using the muleislice method

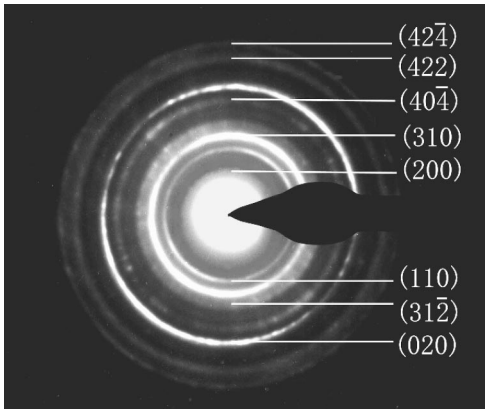

FIG. 3. SAED pattern taken from a sample containing many nanowires.

of Cowley and Moodie[13] and the HRTEM module of the CERIUS2 program[14] for a primary beam energy of 200 kV and a spherical aberration coefficient of $C_s = 1.2$ mm. $K_2Ti_6O_{13}$ compound processes layered structures, which consist of TiO_6 octahedrons joined by sharing edges and corners. K^+ ions are located between the layers. In addition to the simple layered structures, tunnel structures are formed by connecting corners of opposing octahedrons to link the layers together, which can be seen from the atomic models shown in Figs. 5(b) and 5(d). Figure 5(a) is an experimental HREM image recorded along the [001] direction which is consistent with the atomic model shown in Fig. 5(b). The simulated image (inserted in the experimental image and indicted by an arrow in the figure) was obtained using a defocus value of $\Delta f = -150$ Å. The simulated image agrees well with the experimental image. Figure 5(c) is another HREM image recorded along the [1, 11, 6] zone axis. As indicated in this figure, the angle between crystal plane $(11\bar{2})$ and $(60\bar{1})$ is about 73.5°. The inserted simulated image corresponds to a defocus value of $\Delta f = -300$ Å which is seen to agree again excellently well with the experimental image.

B. Growth

In order to understand the growth mechanism, a series of HREM images were recorded for different times of hydrothermal reaction, and the results are shown in Fig. 6. Figure 6(a) is a low magnification TEM image of the raw TiO_2 sample (anatase phase) showing that the sample consists of granular crystals having sizes range from 100 to 400 nm. The surfaces of the anatase particles were initially smooth. After reacted with KOH aqueous solution for one day, Fig. 6(b) shows that many protuberances were formed on the surface of the anatase particle. The higher magnification TEM image [Fig. 6(c)] reveals that the structure of the protuberance is the same as that of the nanowires. We conclude therefore that the nanowires grew out directly from the anatase particles. Figure 6(d) is a HREM image showing the crystalline structure of the anatase particle and its surface protuberances. This HREM image shows clearly that two phases coexist toward the surface of the particle. The structure toward the bulk of the particle shows a smaller crystal plane spacing of 3.5 Å which corresponds to the (101) plane spacing of the anatase phase of TiO_2. The other structure appearing toward the surface of the particle has a larger lattice spacing of about 7.7 Å which corresponds to the (200) plane spacing of $K_2Ti_6O_{13}$. This second phase around the surface of the TiO_2 particle can be regarded as a ''nuclei'' of $K_2Ti_6O_{13}$. After two days of reaction the small protuberances grow bigger to form many thin platelets on the surface of the particles [see Fig. 6(e)]. The crystal platelet has basically a V shape. The tip of the crystal platelet is about several nanometer while the base is about 30 nm. Shown in Fig. 6(f) is a HREM image of a thin crystal platelet, and from this HREM image we can derive the conclusion that the thin crystal platelet is indeed $K_2Ti_6O_{13}$. The thin crystal platelet may further grow preferentially along the [010] direction and finally become a nanowire.

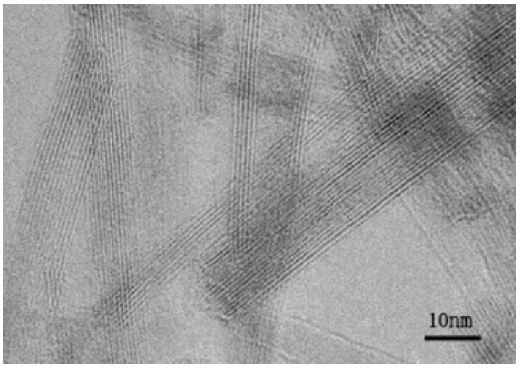

FIG. 4. HREM image showing the layered structure of the nanowires with a layer spacing of 7.7 Å .

Detailed analysis of images such as Fig. 6(d) and corresponding electron diffraction patterns show that the grown $K_2Ti_6O_{13}$ nanoscale crystallites and the parent TiO_2 particles satisfy the following crystallographic relationships:

$$TiO_2(101)//K_2Ti_6O_{13}(200),$$

$$TiO_2[010]//K_2Ti_6O_{13}[010],$$

i.e., the $K_2Ti_6O_{13}$ nanowires grow mainly along the [010] direction on the surface of the parent TiO_2 particles, with their (200) lattice plans parallel to the (101) lattice planes of TiO_2.

Shown in Fig. 7(a) is an atomic model of a $K_2Ti_6O_{13}$ viewed along the [010] zone axis, and in Fig. 7(b) is that of a TiO_2 crystal viewed along the same orientation. As determined experimentally, the (200) lattice planes of $K_2Ti_6O_{13}$ are parallel to the (101) planes of TiO_2, and both are shown to lie horizontally in Figs. 7(a) and 7(b). A schematic model may be constructed as shown in Fig. 7(c) by joining the two (010) surfaces of $K_2Ti_6O_{13}$ and TiO_2 together. It should be pointed out, however, that the lattices of the two compounds are not perfectly matched. The (101) plane spacing of TiO_2 crystal is 0.35 nm, while that of the (200) spacing of $K_2Ti_6O_{13}$ is 0.77 nm. The misfit between the two sets of lattice planes is given by

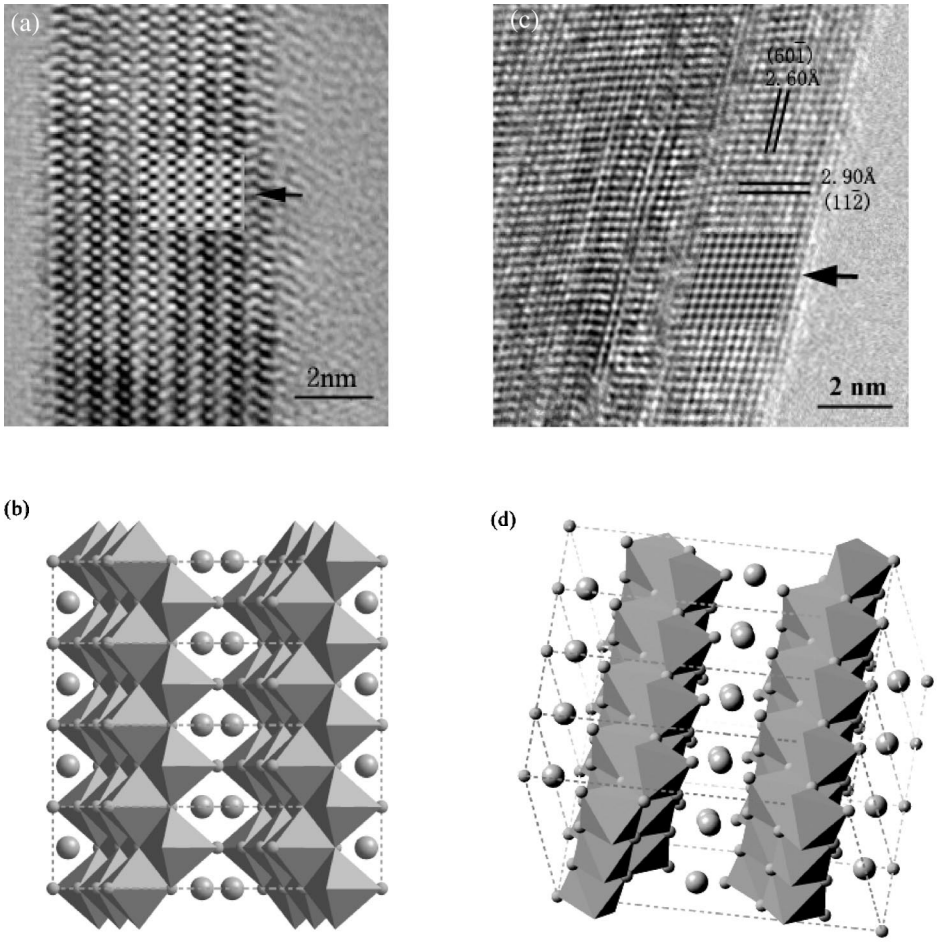

FIG. 5. (a) HREM image showing a nanowire viewed along [001] and (b) corresponding atomic model. (c) HREM image showing a nanowire viewed along [1, 11, 6] and (d) corresponding atomic model. The inserted images in (a) and (c) are simulated images, and both models are built and image simulations are carried out using CERIUS2 software.

$$\delta = \frac{2d_{101} - d_{200}}{(2d_{101} + d_{200})} \approx 9\%,$$

i.e., there exists a large strain associated with the growth of $K_2Ti_6O_{13}$ on the (010) face of TiO_2 along the [010] direction. We expect that the lateral dimension of the grown $K_2Ti_6O_{13}$ crystal will be restricted by the strain associated with the lattice mismatch, which provides in turn a nature selection on the diameter of the grown nanowires.

C. Optical property

Optical measurements in the UV-visible range have been made in order to obtain clues regarding the electronic structure of the potassium titanate nanowires. Shown in Fig. 8 is a typical UV-visible absorption spectrum (solid line) of the nanowires measured using powder samples and a UV-VIS-NIR recording spectrophotometer (Shimadzu UV-3100), together with that obtained from the raw TiO_2 particles (dash line) of the anatase phase and a bulk sample of $K_2Ti_6O_{13}$ (dot line). Our sample of potassium titanate nanowires is indeed a mixture of nanowires and raw TiO_2 particles, but the TiO_2 particles were consumed during the growth of the nanowires. Both XRD and TEM observations suggest that the content of the unconsumed TiO_2 is less than 2% in our final nanowire products. We expect therefore that the solid curve of Fig. 8 reflects the true absorption behavior of the nanowires.

The λ_{onset} of the spectrum recorded from a bulk $K_2Ti_6O_{13}$ sample is about 370 nm. This value is smaller than the onset wavelength of TiO_2 particles with the anatase phase, which is about 400 nm corresponding to a band gap of 3.2 eV. The λ_{onset} of nanowires is seen to be nearly the same as that of the bulk $K_2Ti_6O_{13}$ sample while the shapes of the spectra are obviously different. The effective band gap as derived from the absorption spectra is by definition the energy necessary to create an electron (e^-) and hole (h^+) pair. In principle the excited electron-hole pair forms a bound state, i.e., Wannier exciton, and the behavior of the exciton may be calculated using a ''confined exciton'' model[15] which gives an increase in the apparent band gap energy. The band gap may be estimated from the absorbtion spectra by a linear fit of the square root of the absorption coefficient as a function of the photon energy near the band gap (this procedure is strictly valid only for direct band gaps)

$$\alpha = \sqrt{h\nu - E_g}/h\nu,$$

where $h\nu$ is the corresponding phonon energy. For a given wavelength λ of the phonon measured in nanometer, the phonon energy is given by this procedure gives $E_g = 3.22$ eV for TiO_2 and $E_g = 3.45$ eV for $K_2Ti_6O_{13}$ of both

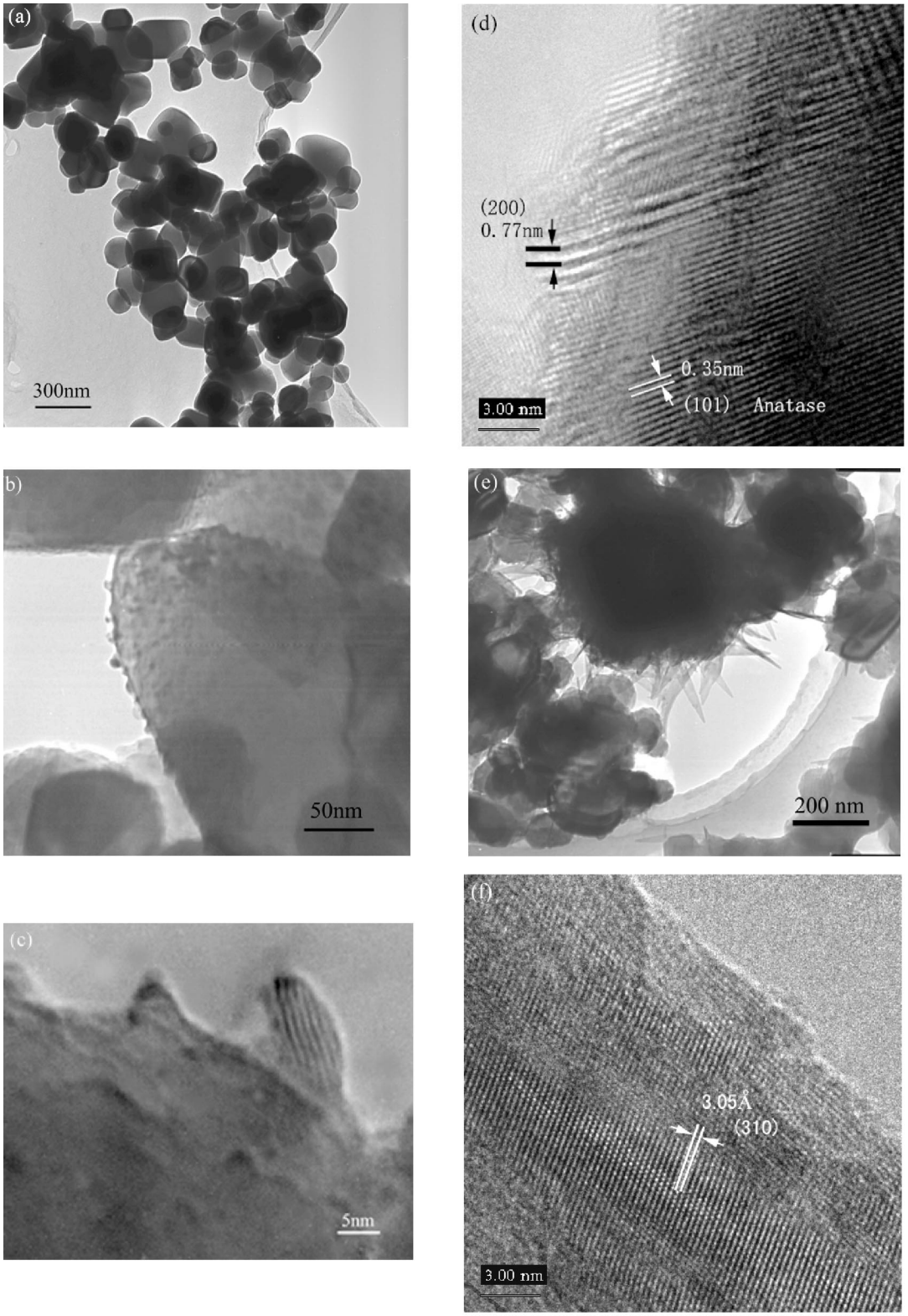

FIG. 6. A series of TEM images showing the growth process of the nanowires. (a) Raw TiO_2 particles with smooth surfaces, (b) many protuberances appearing on the surface of a particle when reacted with KOH for one day, (c) HREM image of a protuberance showing its structure is the same as that of the nanowires. (d) HREM image of a particle showing the orientation relation between the ''nuclei'' of the $K_2Ti_6O_{13}$ nanowire and the anatase matrix, (e) low magnification TEM image showing many thin crystal platelets grow out from a TiO_2 particle, and (f) HREM image of a thin crystal platelet showing its structure is the same as that of the $K_2Ti_6O_{13}$ nanowires.

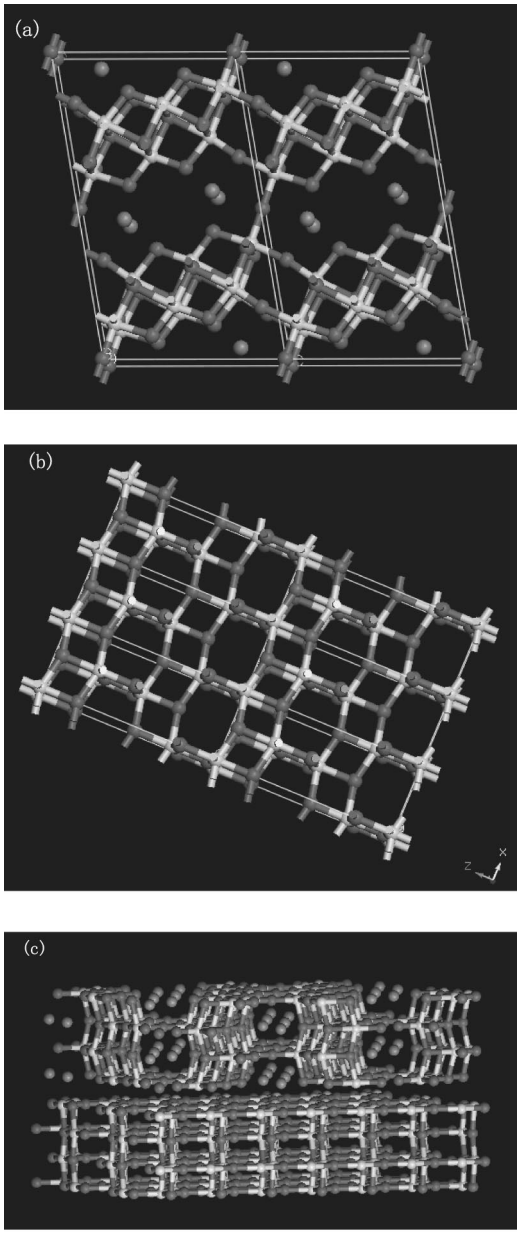

FIG. 7. (a)[010] view of $K_2Ti_6O_{13}$, with (200) lattice planes lying nearly horizontally. (b) [010] view of TiO_2 crystal of anataze phase with (101) lattice planes lying horizontally. (c) A schematic model for the $K_2Ti_6O_{13}/TiO_2$ interface.

raw materials and nanowires. The spectrum obtained from the nanowire sample is also seen to have been enhanced

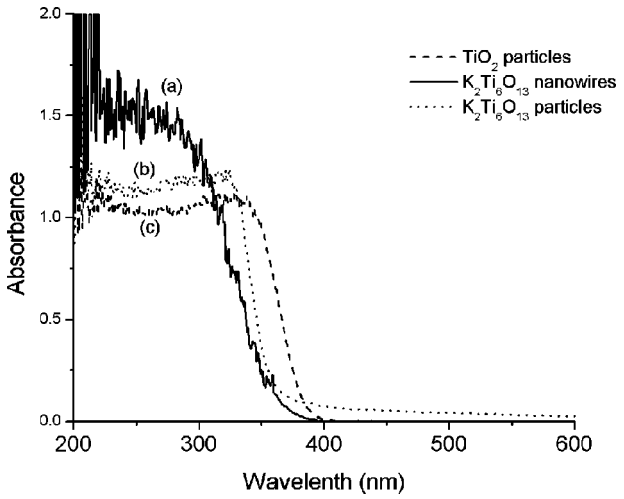

FIG. 8. Experimental UV-visible absorption spectra obtained from (a) nanowires sample, (b) bulk $K_2Ti_6O_{13}$ sample, and (c) a sample containing TiO_2 particles of anatase phase.

toward the shorter wavelength region. This effect might result, among other possibilities, from quantum size effects,[16] following the general trend exhibited by semiconducting nanoparticles.

IV. SUMMARY

We have synthesized titanate nanowires with narrow diameter distribution centered around 10 nm by one step hydrothermal syntheses. Comprehensive structural investigations using XRD and TEM and computer simulations show that the nanowires have the same structure as that of $K_2Ti_6O_{13}$. Experimental evidences are presented which suggest that crystalline $K_2Ti_6O_{13}$ particles were first formed inside the anatase matrix of the TiO_2 particle and then grew out mainly along the [010] direction to develop into the one-dimensional nanowire. UV-visible absorption experiments suggest that the nanowire is a semiconductor with a band gap of about 3.45 eV.

ACKNOWLEDGMENTS

This work was supported by the Ministry of Science and Technology (Grant No. 001CB610502), National Science Foundation of China (Grant No. 90206021), Chinese Academy of Sciences and Peking University.

*Author to whom correspondence should be addressed. Email address: plm@ele.pku.edu.cn or lmpeng@blem.ac.cn

[1] A. Bachtold, P. Hadley, T. Nakanishi, and C. Dekker, Science **294**, 1317 (2001).
[2] Y. Huang, X.F. Duan, Y. Cui, L.J. Lauhon, K.H. Kim, and C.M. Lieber, Science **294**, 1313 (2001).
[3] R. Martel, T. Schmidt, H.R. Shea, T. Hertel, and P. Avouris, Appl. Phys. Lett. **73**, 2447 (1998).
[4] G. Dagan and M. Tomkiewicz, J. Phys. Chem. **97**, 12 651 (1993).
[5] A. Fujishima and K. Honda, Nature (London) **238**, 37 (1972).
[6] K. Fukushima and I. Yamada, J. Appl. Phys. **65**, 619 (1989).
[7] J.H. Li, X.G. Ning, H.Q. Ye, J. Pan, and H. Fukunaga, J. Mater. Sci. **32**, 543 (1997).
[8] K. Suganyma, T. Fujita, K. Niihara, and N. Suzuki, J. Mater. Sci. Lett. **8**, 808 (1989).

[9] J.K. Lee, K.H. Lee, and H. Kim, J. Mater. Sci. **31**, 5493 (1996).
[10] G.H. Du, Q. Chen, R.C. Che, Z.Y. Yuan, and L.-M. Peng, Appl. Phys. Lett. **79**, 3702 (2001).
[11] E. Andersen, I. Andersen, and E. Skou, Solid State Ionics **27**, 181 (1988).
[12] G.L. Li, G.H. Wang, and J.M. Hong, J. Mater. Sci. Lett. **18**, 1865 (1999).
[13] J.M. Cowley and A.F. Moodie, J. Appl. Crystallogr. **10**, 609 (1957).
[14] http:www.accelrys.com/cerius2
[15] L.E. Brus, J. Chem. Phys. **80**, 4403 (1984).
[16] F. Consadori and R.F. Frindt, Phys. Rev. B **2**, 4893 (1970).